Click Here for Full Article

Moment release rate of Cascadia tremor constrained by GPS

Ana C. Aguiar,[1] Timothy I. Melbourne,[1] and Craig W. Scrivner[1]

[1]   A comparison of GPS and seismic analyses of 23 distinct episodic tremor and slip events, located throughout the Cascadia subduction zone over an 11-year period, yields a highly linear relationship between moment release, as estimated from GPS, and total duration of nonvolcanic tremor, as summed from regional seismic arrays. The events last 1–5 weeks, typically produce ~5 mm of static forearc deformation, and show cumulative totals of tremor that range from 40 to 280 h. Moment released by each event is estimated by inverting GPS-measured deformation, which is sensitive to all rates of tremor-synchronous faulting, including aseismic creep, for total slip along the North American-Juan de Fuca plate interface. Tremor, which is shown to be largely invariant in amplitude and frequency content both between events and with respect to its duration, is quantified using several different parameterizations that agree to within 10%. All known Cascadia events detected since 1997, which collectively span the Cascadia arc from northern California to Vancouver Island, Canada, release moment during tremor at a rate of $5.2 \pm 0.4 \times 10^{16}$ N m per hour of recorded tremor. This relationship enables estimation of moment dissipation, via seismic monitoring of tremor, along the deeper Cascadia subduction zone that poses the greatest threat to its major metropolitan centers.

Citation: Aguiar, A. C., T. I. Melbourne, and C. W. Scrivner (2009), Moment release rate of Cascadia tremor constrained by GPS, *J. Geophys. Res.*, *114*, B00A05, doi:10.1029/2008JB005909.

1.   Introduction

[2]   The Cascadia subduction zone stretches 1100 km from Cape Mendocino, California, to northern Vancouver Island, British Columbia, and is known from several lines of evidence to rupture margin wide in $M_w \sim 9$ events every 500–600 years [*Atwater*, 1987; *Satake et al.*, 1996; B. F. Atwater and E. Hemphill-Haley, Recurrence intervals for great earthquakes in coastal Washington, paper presented at Geological Society of America Annual Meeting, Salt Lake City, 1997]. Attendant strain accumulation from the 3–4 cm a^{-1} convergence of the Juan de Fuca plate with respect to North America [*DeMets*, 1995; *Miller et al.*, 2001] manifests itself as NE-directed contraction that is readily measurable with GPS (Figure 1). However, in marked contrast to most other seismogenic convergent margins, the Cascadia plate interface has remained largely devoid of shallow thrust faulting over the last century [*Heaton and Kanamori*, 1984; *Savage et al.*, 1991]. This complicates estimating both the landward limit of the seismogenic zone and thus the seismic hazards posed to the metropolitan regions overlying the subduction zone.

[3]   The discoveries of Cascadia slow slip events [*Dragert et al.*, 2001], their periodicity beneath the Puget Sound region [*Miller et al.*, 2002], occurrence throughout Cascadia [*Szeliga et al.*, 2004, 2008], and their correlation with nonvolcanic tremor (NVT) [*Obara*, 2002; *Rogers and*

Dragert, 2003] have enabled the first instrumental measurement of strain release from the Cascadia plate interface. Slow slip events, which manifest themselves in GPS data as transient reversals from contraction to extension, are always with associated tremor [*Rogers and Dragert*, 2003], occur regularly along the length of Cascadia with a characteristic duration of several weeks, and typically accrue 5 mm of transient deformation (Figure 2) [*Szeliga et al.*, 2008]. Both tremor epicenters and slip inverted from transient, GPS-measured deformation locate to the same lower region, downdip of the inferred locked zone, at 25–40 km depth [*Dragert et al.*, 1994; *McCaffrey et al.*, 2007; *Wang et al.*, 2003]. This region lies directly beneath the western margin of the major population centers of Cascadia, such as Seattle, Washington, Portland, Oregon, and Vancouver, British Columbia. The correspondence between GPS-inferred slip and tremor has improved markedly as instrumentation has increased (Figure 3), and the preponderance of evidence now suggests that tremor, whose coda can persist for hours, may be composed of the scattered arrivals arising from many small thrust fault slip events occurring sequentially along the tectonic plate interface. Within the Nankai Trough of Japan, tremor has been shown to be located along the plate interface [*Shelly et al.*, 2007], and to be largely composed of discrete low-frequency earthquake sources [*Shelly et al.*, 2007], each of which shows thrust fault mechanisms with orientations consistent with the direction of the subduction of the Philippine plate beneath western Shikoku [*Ide et al.*, 2007b]. In Cascadia, tremor polarization is also consistent with stick-slip sources in line with local convergence direction [*Wech and Creager*, 2007] and, more recently,

---

[1]Department of Geological Sciences, Central Washington University, Ellensburg, Washington, USA.
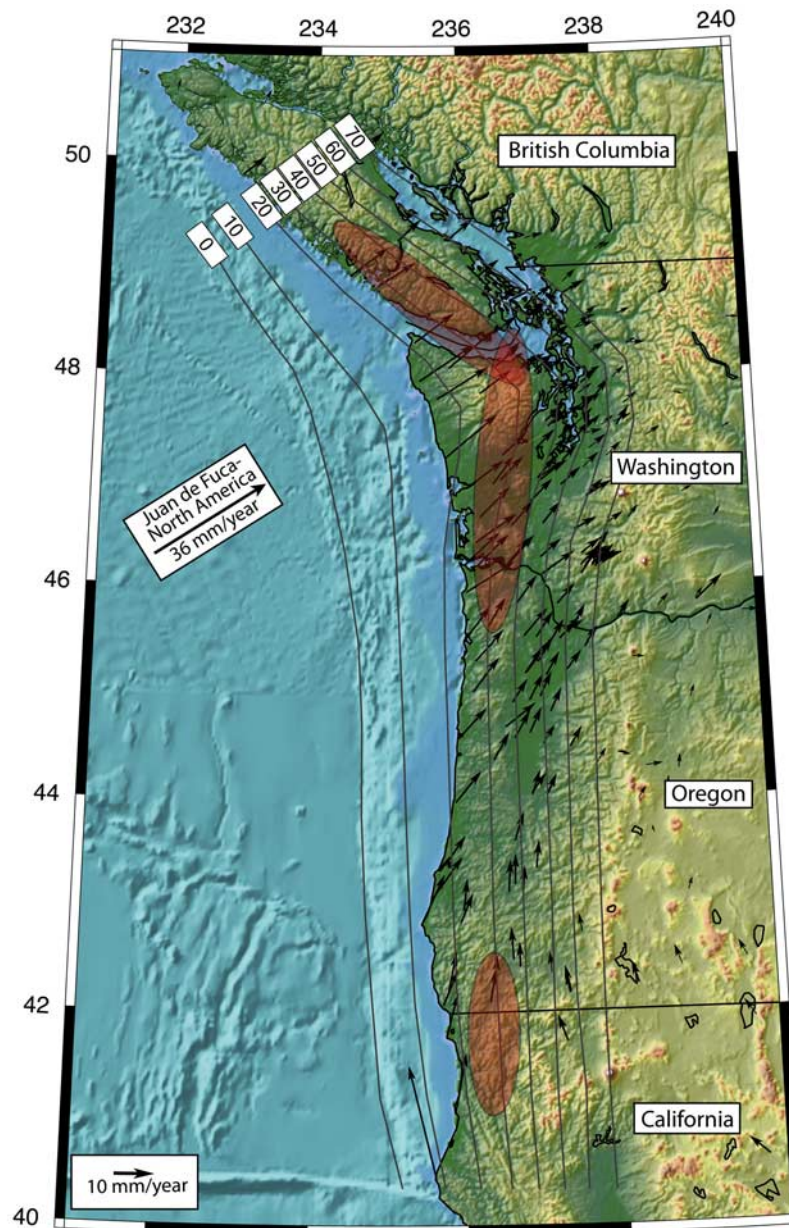
Figure 1. Interseismic deformation (black vectors) of the Cascadia subduction zone, in which the Juan de Fuca plate subducts at between 3 and 4 cm a^{-1} beneath North America, specifically 36 mm a^{-1} beneath northwestern Washington state. Plate interface depth contours are labeled with gray lines (km), and general locations of the 23 slow slip events discussed here are outlined with red ellipses. GPS vectors showing secular deformation come from combined solutions of the Pacific Northwest Geodetic Array [*Miller et al.*, 1998] and the EarthScope Plate Boundary Observatory (http://www.earthscope.org).

some tremor sources that previously were located radially throughout the accretionary wedge have subsequently been shown to locate instead directly along the plate interface [*LaRocca et al.*, 2009]. Together, these results suggest that tremor in Cascadia, as well as the Nankai Trough, arises from stick-slip faulting that must dissipate moment from the deeper plate contact. Episodic tremor and slip (ETS) [*Rogers and Dragert*, 2003] is, therefore, widely assumed to dissipate strain energy accumulating from ongoing convergence along the deeper region of the plate interface.

[4] Quantifying the rate of moment release during tremor remains elusive, however, for a host of reasons. Most fundamentally, the proportion of moment that is expressed in the seismically detectable tremor bands, typically 2–10 Hz, versus longer-period or purely aseismic faulting, is unknown. Preliminary analyses have suggested that only a small fraction of total moment is released as seismically detectable tremor [*Houston*, 2007; *Ide et al.*, 2008]. Moreover, the waveform characteristics of tremor exacerbate the difficulties of moment estimation as well. In Cascadia, individual tremor
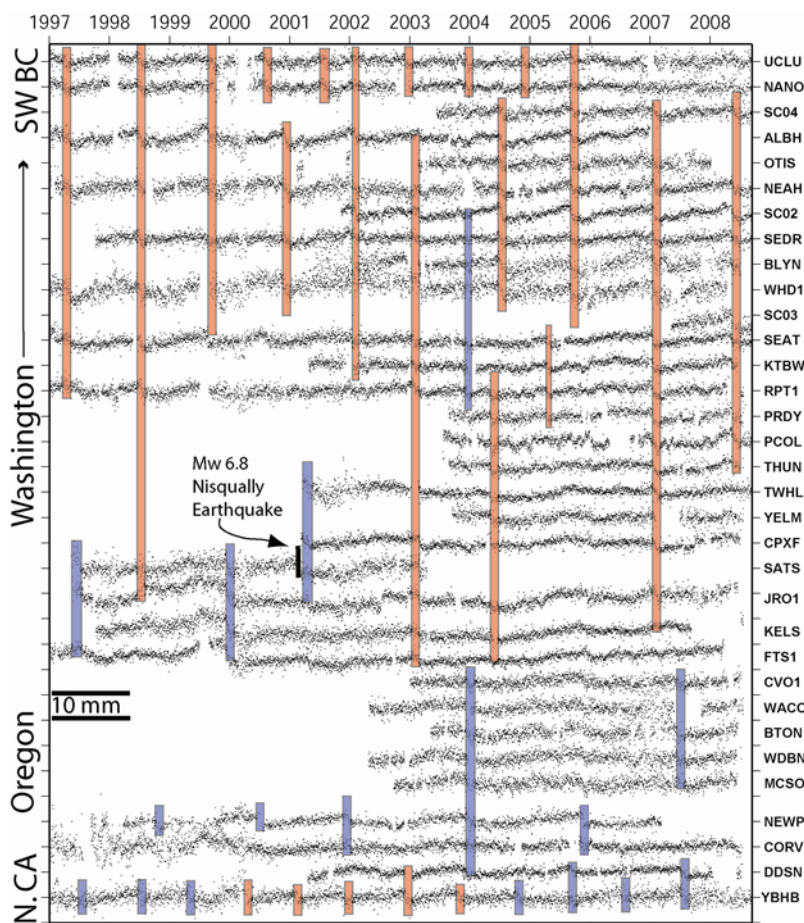
Figure 2. The 11 years of GPS longitude measurements from the Cascadia subduction zone show evidence of 39 slow slip events. Vertical axis tick marks are 10 mm. Transparent blue and red lines indicate slip events well recorded with GPS or corroborated by observations of subduction zone tremor; red lines denote events for which tremor duration could be estimated either with available digital data or via published reports based on analog data. Maximum geodetic offsets observed to date measure 6 mm and correspond to the spatially largest event in early 2003. The February 2001 M_w 6.7 Nisqually earthquake (depth = 52 km) appears on station SATS. Station map can be found at http://www.geodesy.org.

bursts vary in duration by over 6 orders of magnitude, from a few seconds to several days without interruption. While tremor amplitude can vary by a factor of 10 between individual bursts within a given episode, the majority of all bursts, which can occur minutes or hours apart, have average peak velocities that typically range between 15 and 300 nm s^{-1} (Figures 4 and 5). More importantly, neither the amplitude nor dominant frequencies of tremor vary in any systematic fashion throughout the subduction zone, or with respect to individual burst durations (Figure 4). This invariance is markedly different from that of regular earthquakes and eliminates all traditional seismic magnitude estimation techniques from assessing their moment release. Finally, although tremor shows a high degree of temporal correspondence with GPS slip inversions during the 2005 and 2007 events, there remains the noted difficulty in accurately locating tremor [*Kao et al.*, 2005; *McCausland et al.*, 2005]. Without the ability to directly measure moment release during tremor, it is impossible to quantify the extent to which

these events dissipate, over the long-term, strain energy accumulated by ongoing convergence.

[5] For Cascadia, however, moment release can be inferred from joint GPS and tremor monitoring of ETS. This region has long been instrumented with both GPS [*Miller et al.*, 1998] and seismic networks, which permit a unique opportunity to calibrate moment release during tremor events through time. Because the GPS-determined transient near-field deformation is sensitive to all fault slip, regardless of rate, the geodetic inversions for moment sidestep the spectral content unknowns of tremor by providing a comprehensive estimate of all moment released during a given event, including that from transient aseismic creep. Even if the tremor wavefield constitutes only a small portion of the total moment released in a given event, if that proportion is constant over many events and areas, then tremor, once empirically related to GPS-inverted moment release, can be used as a proxy for moment release, particularly for smaller tremor bursts of only a few hours that cannot be observed with GPS.
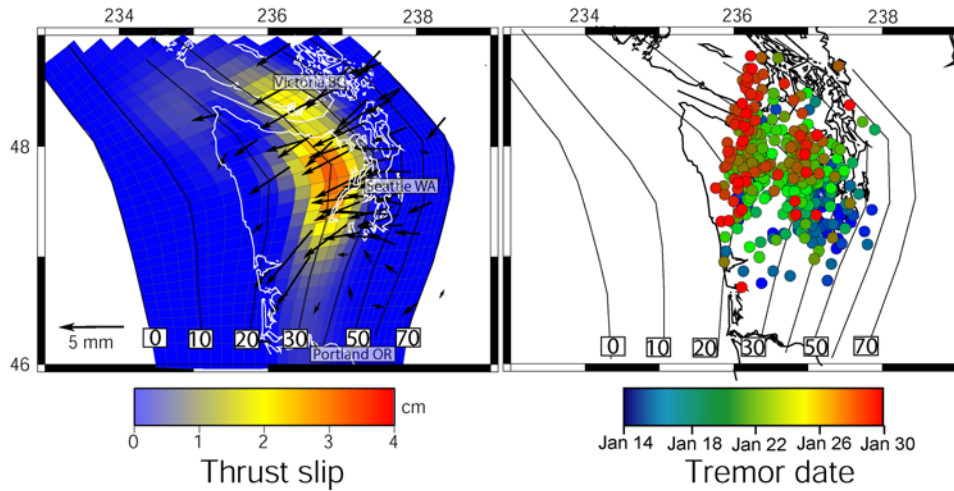
Figure 3. Slip distribution and tremor locations of the January 2007 Cascadia ETS event. (left) Black arrows show horizontal deformation of 83 GPS stations that bracket the observed deformation. Thrust faulting of up to 4 cm inverted from the GPS is clustered around the 30–40 km depth contour, and the moment calculated for this event gives M_w 6.7. (right) Circles show 450 separate tremor bursts using location scheme described in the text and colored according to date of occurrence. Events correspond well in map view to slip inverted from GPS, but hypocentral depths are widely scattered.

[6] This approach is motivated in part by the uniformity of tremor and GPS transients seen to date in Cascadia: all observed GPS reversals have been correlated with major tremor episodes; no GPS reversals during which seismic recordings are available have been observed without at least 70 h of simultaneous tremor; and no large tremor episodes (>70 h) have been observed without accompanying transient GPS deformation. However, smaller episodes ranging from a few seconds to a few tens of hours are routinely observed without resolvable GPS or strainmeter signals. These can contribute upward of one third of total tremor observed over a multiyear time scale, and thus presumably moment release as well [*Aguiar et al.*, 2007; *Kao et al.*, 2008; *Wech and Creager*, 2008]. This paper thus offers a GPS-calibrated method of quantifying the moment release associated with tremor bursts of all durations within the Cascadia subduction zone. This method enables the mapping of moment release from the Cascadia subduction zone that can, in turn, be used to assess
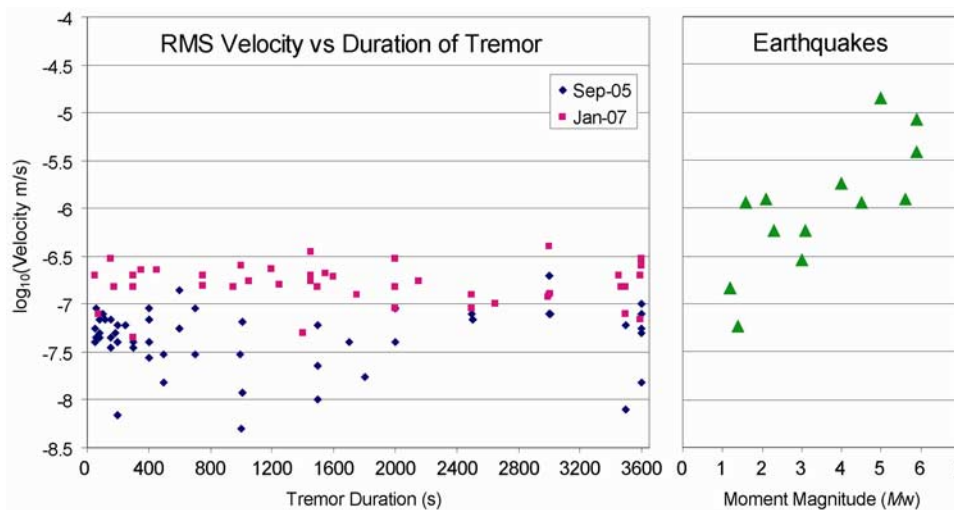

Figure 4. Network-averaged amplitudes of tremor as a function of tremor burst duration, ranging from a few seconds to 1 h. (left) Blue diamonds represent tremor bursts from the September 2005 event, and pink squares represent tremor bursts from the January 2007 event. Network-averaged tremor amplitude is consistently around 100 nm s^{-1} and does not vary with respect to duration of tremor burst. The average difference between the 2005 and 2007 events is likely due to the tremor hypocentral location relative to the available stations that recorded it; the 2007 event was better recorded. (right) Green triangles show network-averaged amplitudes of regular earthquakes of variable magnitude vary by nearly 3 orders of magnitude, as measured on the same stations as the tremor. By comparison, tremor amplitudes are statistically invariant with respect to burst duration.
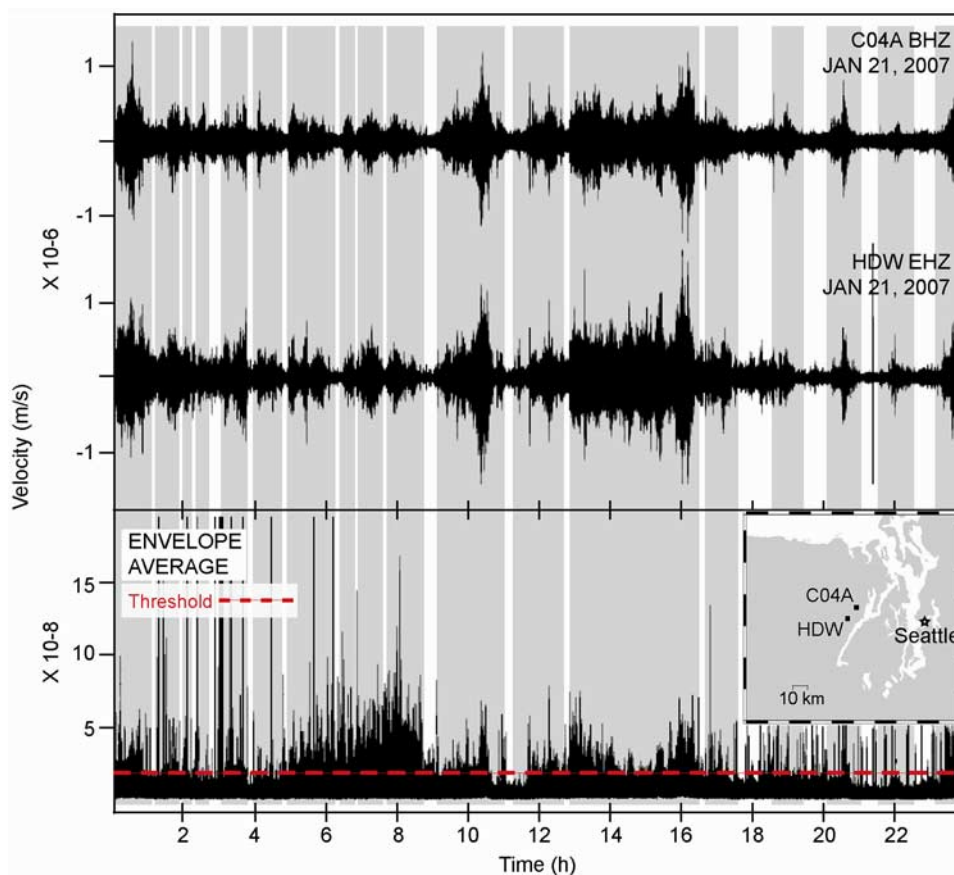
Figure 5. (top) Near-continuous tremor during a 24 hr period from northern Washington state recorded on two different stations located roughly 10 km apart. (bottom) Grey bands show times of ongoing tremor, as picked from networked averages of the signal envelopes. Although tremor bursts vary in duration over 6 orders of magnitude, from a few seconds to whole days, the network-averaged bursts vary little with respect to duration in either amplitude or dominant frequency.

seismic hazards posed by these source regions that lie closest to major metropolitan centers.

2. Nonvolcanic Tremor in the Cascadia Subduction Zone

[7] Cascadia nonvolcanic tremor appears as low-amplitude, band-limited seismic noise that is phase-incoherent when recorded simultaneously across regional seismic arrays of apertures of tens of km. On dense seismic networks (spacing of tens of meters) tremor is phase-coherent between stations, but differentiating between ETS-related tremor and other noise sources can be problematic. It emerges both spontaneously without apparent triggering and through triggering by passing Rayleigh and Love wave trains respectively [*Brodsky and Mori*, 2007; *Rubinstein et al.*, 2007]. In Cascadia tremor can persist for durations ranging from a few seconds to days on end.

[8] Seismic estimates of tremor duration for each of the 23 events captured with GPS were derived from five different sources using a variety of techniques and data, but which produce internally consistent tallies of total tremor for events analyzed with more than one method. Events beneath Vancouver Island were tallied by manual inspection [*Rogers and Dragert*, 2003] and by the TAMS method of

tremor monitoring and location [*Kao et al.*, 2006], which produces tremor estimates that agree to within 10% with manual tremor assessments. For Puget Sound tremor estimates prior to September 2005, we use the results of hours of tremor described by *McCausland et al.* [2005] and *Rogers and Dragert* [2003], which were compiled manually. Tremor from northern California events that occurred between 2001 and 2005 was also tallied by manual inspection of seismic data from the Northern California Seismic Network, the Berkeley Digital Seismic Network, and the IRIS Global Seismic Network during a 1-month time period centered on the event date and was published by *Szeliga et al.* [2004].

[9] For the recent northern Puget Sound events in 2005 and 2007, data were merged from the Pacific Northwest Seismographic Network (PNSN), the EarthScope borehole and transportable array seismic networks and EarthScope CAFE experiment network, during the time span from July of 2005 to February of 2007. Data were merged into daily files, degained and decimated at 10 Hz. Envelope functions were stacked across forearc stations and calculated for each day of the year (Figure 5). We assume that any signal that survives the envelope stack above a noise threshold is tectonic in origin, since local noise should not stack coherently across the array. We determined the noise threshold by comparing envelope stacks between forearc stations known
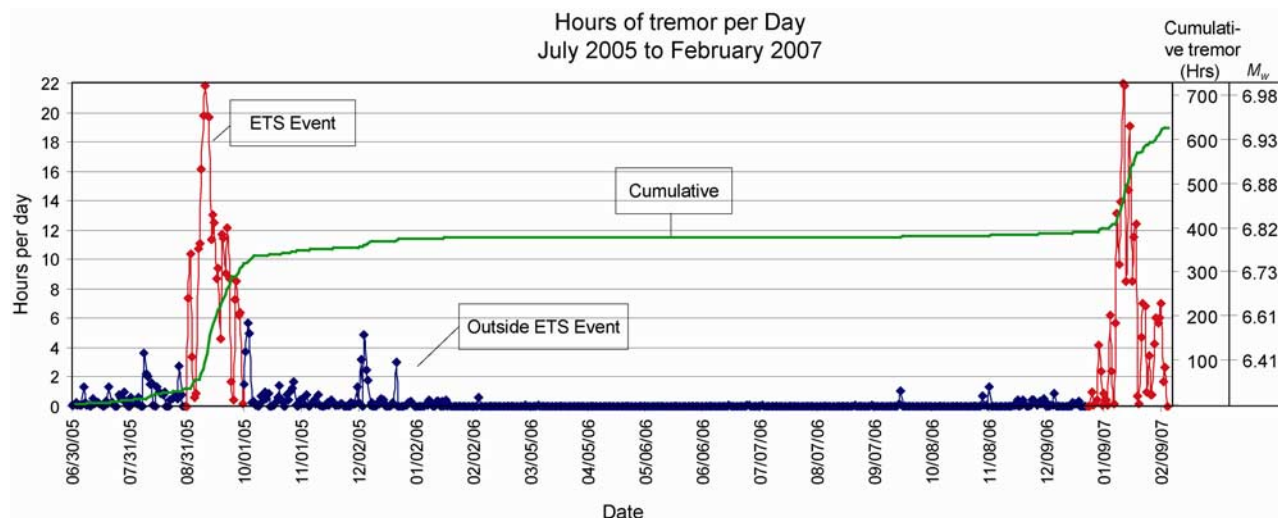
Figure 6. Hours of tremor per day and total cumulative hours of tremor from 30 June 2005 to 11 February 2007. Red lines represent the two ETS events captured by these data, the September 2005 event (284.9 h total tremor) and January 2007 (238 h). Blue lines represent the remainder of the time and show that during 2006 there was relatively little tremor activity. Values for moment magnitude are from the regression scale derived in Figure 7, $M_0/hr = 5.2 \pm 0.4 \times 10^{16}$ N m.

to show tremor with other stations on which tremor is not commonly observed. The threshold is reestimated each day to account for time-dependent background noise variation, but typically averaged around 30 nm s^{-1}, as shown in Figure 5. On this basis the start and stop times of discrete tremor bursts were identified, and durations were found to range from a few seconds up to 20 or more hours in a given episode. Figure 6 shows a plot of tremor hours during ~19 months of data from northern Washington, containing 627.5 h of tremor in total. Of this amount, 284.95 h are from the September 2005 event and 238.38 h correspond to the January 2007 event.

[10] In addition to the largest events that are detectable with GPS, smaller bursts of tremor are distributed randomly throughout the time period in question and constitute roughly 20% of the total observed tremor during this particular 19-month time period. This number is corroborated by Kao et al. [2008] using tremor identified over a 10-year time period that includes all of Vancouver Island. Wech and Creager [2008], however, find that during a 15-month time period that includes the 2007 and 2008 events beneath western Washington state, closer to half of total tremor occurred between the events and half in the 2007 and 2008 events themselves. This discrepancy either suggests that the three tremor detection algorithms have differing thresholds for the shorter-duration bursts that occur between the major events, or that the two time periods, September 2005 to February 2007, and January 2007 to June 2008, showed different amounts of low-level tremor.

[11] For the events analyzed with this technique, however, the various approaches give similar answers to each other as well as to tremor identified manually by eye. For the subset of the 23 events discussed here that were tallied by multiple groups, either manually, with the TAMS method or by stacking envelopes, the agreement between the different methods is in all cases less than 10%. For the 2007 and 2008 events the difference between these three methods is closer to 5%.

[12] It is important to note that ETS-related tremor is differentiated from wind, ocean wave, and anthropogenic noise "tremor" by the spatial scale over which it is observed: in some cases as much as several hundred km for higher-amplitude bursts. All of the tremor counting approaches used to tally total tremor durations in this study, manual inspection [Rogers and Dragert, 2003], the TAMS method [Kao et al., 2006], the McCausland et al. [2005] approach of two dense arrays, and the stacking method outlined above, involve station spacing of a minimum of tens of km, over which non-ETS noise is presumed to not stack coherently. Highly dense arrays composed of many stations grouped tens of meters apart, by contract [Sweet et al., 2008] will record ETS tremor at a much lower amplitude, and presumably more of it through time, than will a regional seismic array analysis, but it will also record non-ETS noise sources with little ability to discriminate ETS tremor from non-ETS noise. The tremor threshold used here, and thus the moment release rate it provides, is appropriate only for regional seismic array analysis over which the stations are spread tens of km.

[13] The uncertainty of the total duration of tremor estimated for each event is difficult to quantify given the variable methodologies used, and for those events whose tremor was tallied manually no estimate of uncertainty is available. For the purposes of computing a moment tremor duration regression curve, we assign an uncertainty (1σ) in tremor duration of 10% of total tremor, which is the upper bound of disagreement between the tremor tallies for events analyzed by all three methods.

3. Tremor Locations

[14] Tremor locations for the 2007 event (Figure 3) were computed by picking the maximum amplitude of distinct bursts that were coherent across the available stations, rather than cross correlating smoothed envelopes of data [McCausland et al., 2005; Obara, 2002; Wech and Creager,

2008]. A three-dimensional grid was then searched for the location that minimized the L2 norm of misfit between observed differential travel times and that predicted for each potential location using a 1-D shear velocity model appropriate for Cascadia. As with previous estimations, tremor locations generally agree in map view with the geodetically inferred region of slip between 25 and 40 km depth. The hypocentral depths, however, are widely varying and, more importantly, are unstable with respect to the time picks. A slight variation in differential times picks on one or more stations produces widely varying depths for a given burst without significant changes in horizontal location (as is expected for differential time analyses). We therefore consider the tremor depths to be unconstrained by this location scheme and assume that, as in the Nankai Trough [*Shelly et al.*, 2007, 2006], Cascadia tremor also originates from the plate interface.

[15] To assess the extent to which the amplitude of tremor varies with respect to its duration, the network-averaged tremor bursts were binned into discrete length windows ranging from 10 to 3600 s. Windows longer than 1 min were also performed and represented as 3600 s for easier illustration. The amplitudes of the stacked data were then averaged over the duration of each tremor burst in each bin for the September 2005 and January 2007 ETS events. While individual tremor bursts do vary in amplitude through time (Figure 5), the majority of bursts within a particular event (e.g., September 2005) typically vary by less than a factor of 10 during the event, and show no clear or statistically significant dependency on burst duration (Figure 4). There is some evidence of average amplitude differences between the 2005 and 2007 events, but this is consistent with the primary locus of faulting of the 2005 event, as inverted from the GPS measurements, being more distant from the seismic stations that best show NVT than that of the 2007 event. For all tremor durations over both events, the array-averaged velocities were tightly clustered around 100 nm s^{-1}. Like the amplitude, the dominant frequencies of tremor were also not observed to vary with respect to duration: FFTs of tremor bursts from discrete bins of separate duration were compared and no obvious or statistically significant trends in tremor frequencies as a function of duration were observed.

4. GPS Constraints on Cascadia ETS Moment Release

[16] To estimate moment release during Cascadia ETS episodes, raw GPS phase observables from the combined networks of the Pacific Northwest Geodetic Array, Western Canada Deformation Array and Plate Boundary Observatory were processed with the GIPSY (Zumberge) software package as described by *Szeliga et al.* [2008]. The resultant time series of Cascadia GPS positions relative to cratonic North America were then decomposed into a set of basis functions that include linear trends, annual and semiannual sinusoids, and a summation of step functions introduced at times of known earthquakes, slow earthquakes, or GPS instrumentation upgrades. This approach of simultaneous decomposition yields the full covariances of all estimated parameters and the east component of transient deformation due to the slow slip events discussed here is shown in Figure 2.

[17] To invert for slip we specify the plate boundary surface by linearly interpolating between depth contours supplied by *Flück et al.* [1997]. This surface is then divided into variable sized subfaults whose typical dimensions are approximately 25 km along strike and 15 km downdip. We enforce positivity (thrust-only slip) in the inversion by employing the nonnegative least squares algorithm of *Lawson and Hanson* [1995]. To avoid highly oscillatory and non-unique slip distributions, we implement smoothing by row augmenting the matrix of Green's functions with a finite difference approximation to the Laplacian operator and augmenting the corresponding rows of the data vector with an equal number of zeros. This requires finding an optimum weighting factor to control the degree of smoothing, which is achieved by solving a data-reduced vector and constructing a bootstrap estimate of the remaining data to predict the missing data subsets [*Efron and Tibshirani*, 1994]. Although smoothing trades off with maximum slip, the resultant moment inverted from the transient data is largely invariant with respect to smoothing, and changes the estimated moment by less than 15 percent over 4 orders of magnitude change in the smoothing parameter [*Szeliga et al.*, 2008]. Because of this, uncertainty of the GPS-based estimate of moment release stems not from the degree of smoothing, but rather from the uncertainties of the transient offsets estimated from the geodetic time series. These are typically 1, 2 and 4 mm in north, east and vertical components, and which are presumably random across the GPS array. Experiments in which the estimated transient deformation was altered with random perturbations to the estimated offsets of these noise amplitudes changed the estimated moment for each event by never more than 1×10^{18} N m which we therefore use as the uncertainty (1σ) in computing the moment tremor duration regression curve. For one small event in November of 2006, the moment was estimated by modeling transient strain recorded on borehole strainmeters on southwestern Vancouver Island that was accompanied by ~70 h of tremor [*Wang et al.*, 2008].

[18] Figure 3 shows the geodetic displacements and slip distributions for the January 2007 event. To get the locations shown in Figure 3, we high-pass filtered the data at 1 s, computed the envelopes, and low-pass filtered those at 10 s. With these we manually picked tremor burst peaks that coincided at a minimum of five stations. Last we calculated the observed travel times between the pairs of stations. The location was determined by minimizing the L2 norm of the measured differential travel times minus the predicted differential travel times calculated from a 1-D S wave velocity model on a cube grid.

5. Moment Rate During Nonvolcanic Tremor

[19] Comparing the GPS-estimated moment release for each event with the duration of recorded tremor shows that they are highly correlated. Figure 7 shows moment estimates for the 23 largest events, which span the Juan de Fuca-North American plate interface over a 10-year period, versus the cumulative hours of tremor measured for each event. The best fitting rate is

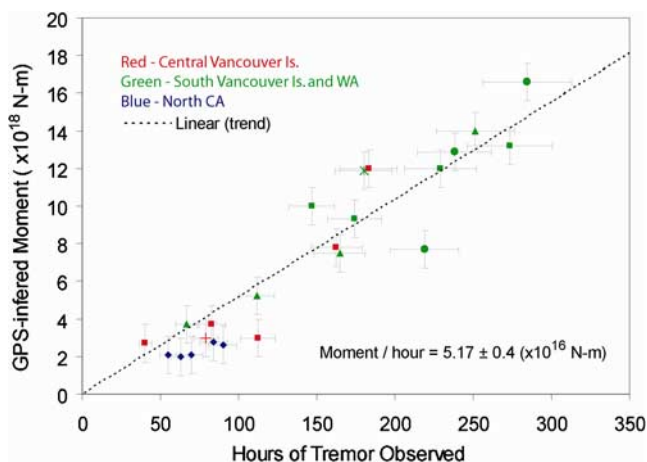$$M_0/\mathrm{hr} = 5.2 \pm 0.4 \times 10^{16} \mathrm{N-m/hr},$$

Figure 7. Cumulative hours of tremor for each of 23 distinct Cascadia ETS events plotted against moment release, as estimated by inverting GPS measurements of transient deformation for thrust slip along the Juan de Fuca-North American plate interface. Moment and tremor for an additional small event recorded on a borehole strainmeter was drawn from *Wang et al.* [2008]. Symbol type delineates source of tremor duration, which includes both manual and automated counting methods: Circles, this study; triangles, *McCausland et al.* [2005]; crosses, *Rogers and Dragert* [2003]; squares, *Kao et al.* [2007]; plus, *Wang et al.* [2008]; diamonds, *Szeliga et al.* [2004]. Colors represent the area in which the ETS occurred: red is central British Columbia, green is southwestern British Columbia and northern Washington, and blue is northern California. Tremor uncertainties are assumed to be 10% of total tremor; moment uncertainty is 1×10^{18} N m (see text for details). See Figure 1 for map view of ETS locations. Best fit moment rate function is $5.2 \pm 0.4 \times 10^{16}$ N m per hour of recorded tremor.

or

$$M_0/s = 1.4 \pm 0.1 \times 10^{13} \text{N} - \text{m/s}.$$

It should be noted that this regression curve is tied de facto to the origin (no tremor implying no moment release), but even without this constraint the data nonetheless indicate that zero hours of tremor correspond to no moment release within the error of the regression curve. The data points cluster tightly around the linear trend, with a 2σ uncertainty on the moment rate that is less than 10% of the rate itself, despite the wide geographic range of events included in the data set.

[20] The 23 events in Figure 7 include only the largest events seen in Cascadia: those with GPS deformation of several mm, moment magnitudes of 6.3 to 6.8, and 40 to 280 h of tremor. The moment magnitude for the smallest included events, magnitudes of ∼6.3, appear as roughly 2 mm of deformation at the earth's surface, the smallest signal resolvable with GPS. Shorter-duration tremor bursts, those less than typically ∼70 h, likely deform the surface at levels too small to be observed with GPS, but have been resolved with borehole strainmeters [*Dragert et al.*, 2007]. These smaller bursts presumably also dissipate

moment, and the linearity of this relationship over the range of larger events suggests the scale can be extrapolated to smaller-duration tremor bursts. These smaller bursts, typically lasting a few days and producing less than ∼50 h of tremor, are routinely observed throughout the arc and have been shown to constitute between 20 and 50% of the total tremor recorded in the central Puget Sound region and Vancouver Island [*Aguiar et al.*, 2007; *Kao et al.*, 2008; *Rogers and Dragert*, 2003; *Wech and Creager*, 2008]. Other than duration, these shorter-duration tremor bursts are otherwise indistinguishable, in terms of amplitudes and frequencies, from their longer-lived counterparts. Table 1 shows moment magnitude values calculated using the moment magnitude-tremor time model for different tremor durations, ranging from 250 h down to a few minutes.

6. Discussion

[21] It is surprising that all well-recorded Cascadia ETS events along most of the arc are consistent with a single, linear scaling between moment release and duration of recorded tremor, particularly given its length of nearly 1100 km over which coupling presumably varies significantly along strike [*McCaffrey et al.*, 2007; *Mitchell et al.*, 1994]. The events included here, those for which both GPS and seismic data are available; include northern California, northernmost Oregon, Washington and southwestern British Columbia. There are gaps along the arc in which either GPS or seismic data are not readily available

Table 1. Values for Different Tremor Times Calculated Using the Magnitude-Time Model[a]

Hours	Moment Magnitude ($M_{\rm w}$)
250	6.68
200	6.61
150	6.53
100	6.41
50	6.21
10	5.75
5	5.54
4	5.48
3	5.40
2	5.28
1	5.08

Minutes	Moment Magnitude ($M_{\rm w}$)
55	5.05
50	5.03
40	4.96
30	4.88
20	4.76
10	4.56
5	4.36
4	4.29
3	4.21
2	4.04
1	3.89

[a]The moment rate function of $5.2 \pm 0.4 \times 10^{16}$ N m per hour of recorded tremor (Figure 8) can be used to quantify the moment release from numerous and ubiquitous smaller tremor bursts that are not resolvable on GPS or strainmeter recordings. 70 h of tremor constitute the equivalent moment of an $M_{\rm w}$ 6.3 event, the smallest resolvable with GPS; 1 h of tremor equals a $M_{\rm w}$ 5.1 event, and 1 min a $M_{\rm w}$ 3.9. This scale enables continuous moment dissipation measurements with high-frequency seismic monitoring.
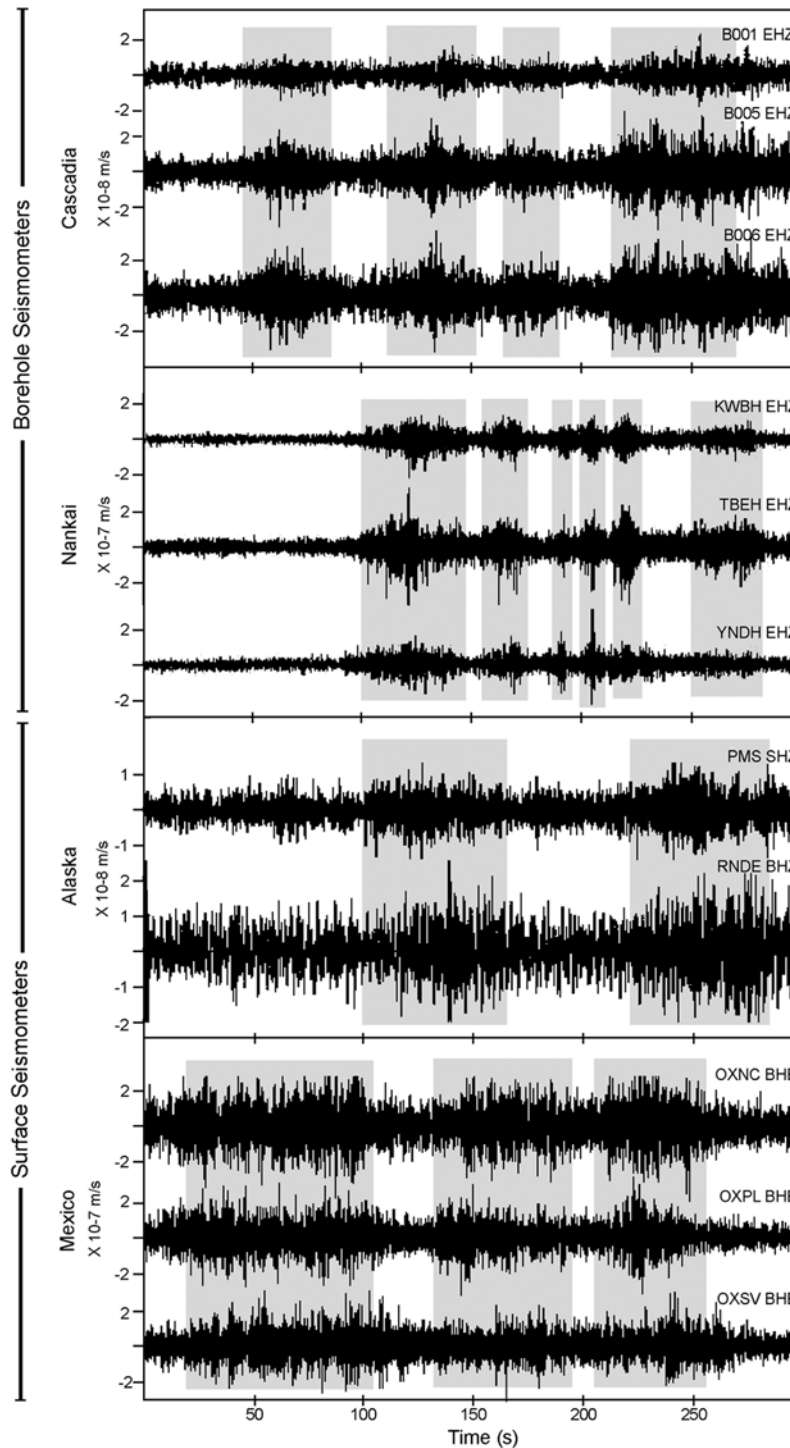
Figure 8. Five minutes of nonvolcanic tremor from four subduction zones. Times of identifiable tremor are shaded in gray and range in duration from a few seconds to several hours. All tremor consistently shows velocity amplitudes ranging between 100 nm s^{-1} and 10 nm s^{-1} and frequency characteristics of 1–30 Hz. Data from Cascadia and Japan data are borehole recordings and show higher signal to noise, while Alaska and Mexico data are surface recordings. Data provided by Doug Christensen (Alaska), David Shelly (Japan), and Michael Brudzinski (Mexico).

and for which a comparison cannot yet be made, most notably throughout central Oregon between 44 and 46°N, but in those regions that do contain both measurements the observed relationship holds. It is also plausible that other processes, such as aseismic creep, may be present, but any long-period or aseismic moment release is recovered by GPS and thus must represent a consistent bias from event to event within the moment calibration.

[22] The linearity of the tremor duration-moment magnitude relationship throughout the arc suggests that in those regions that do show tremor, the rate of moment release is consistent from arc segment to segment, and through time, at least for the past decade in the Cascadia subduction zone. It also implies that the proportion of total moment released as tremor, versus that released as longer-period seismicity or aseismic moment, is also constant through time and across the plate interface. This must therefore represent an important constraint on the constitutive properties of the deeper region of plate interfaces that can radiate seismic energy within the tremor frequency band. This points toward a frictional regime likely composed of many small, seismogenic asperities that can slip quickly enough to radiate 1–10 Hz seismic energy, but which must also be damped before growing extensively into a broad-scale rupture. This fault texture, if primarily temperature controlled, may then be consistent throughout the arc, yielding the invariance observed in moment release rate.

[23] It is also possible, though as of yet undetermined, that other subduction zones will show a different proportionality between tremor and released moment. However, Cascadia tremor amplitudes and frequencies are comparable to tremor now documented in many subduction settings that span the known range of convergence rates and subducted plate age, including Mexico, Alaska and Japan [*Brown et al.*, 2005; *Brudzinski et al.*, 2007; *Douglas et al.*, 2005; *Kao et al.*, 2005; *McCausland et al.*, 2005; *Peterson et al.*, 2007; *Szeliga et al.*, 2008] (Figure 8), but as of yet no systematic estimate of moment release as a function of tremor duration has been established for these regions. Also, tremor has been found within continental transform faults in California. In one case, the signal persists for ∼10 min periods and appears to come from 20 to 40 km depth beneath the Cholame region of the San Andreas fault [*Nadeau and Dolenc*, 2005]. In the second case, tremor along smaller strike-slip faults near the San Andreas is observed during the passage of teleseismic surface waves, with durations lasting tens of seconds [*Gomberg et al.*, 2008; *Nadeau and Dolenc*, 2005]. Neither instance is accompanied by resolvable geodetic signals, but if the tremor source here is similar to Cascadia, such signals would not be expected. Using the moment rate derived in Figure 7, these signal durations correspond to $M_w = 4.5$ (at 20–40 km depth) for the Cholame tremor and $M_w = 3.6$ for the off San Andreas faults, which lie well below the resolution of most forms of geodetic measurements, including borehole strainmeters.

[24] In all tectonic settings in which tremor is observed, its characteristics are similar to that seen in Cascadia: velocities are typically several hundred nanometers per second, and rarely exceed maxima of a few microns per second, or those typical of M_w 1 earthquakes, suggesting the moment duration scaling may be applicable outside Cascadia. The tremor moment rate derived here is consistent with the *Ide et al.* [2007a] scaling law of $M_0 = T \times 10^{13}$ N m s^{-1}, which is based largely on events from Japan but which takes into account many different manifestations of slow slip, including low-frequency tremor, low-frequency earthquakes, very low frequency earthquakes, and slow slip events [*Dragert et al.*, 2004; *Ide et al.*, 2007b; *Ito and Obara*, 2006a, 2006b; *Ito et al.*, 2006; *Miller et al.*, 2002; *Rogers and Dragert*, 2003; *Shelly et al.*, 2006].

[25] While time will tell whether the moment tremor duration established here will be more widely applicable outside Cascadia, it does allow moment release from the deeper Cascadia subduction zone to be quantified purely by seismic monitoring with inexpensive, high-frequency seismometers. This, in turn, can be translated into improved estimation of seismic hazards for the metropolitan regions that overlie this part of the plate interface.

References

Aguiar, A. C., T. I. Melbourne, and C. Scrivner (2007), Tremor constraints on moment release during the 2007 ETS from surface and borehole seismometers, *Eos Trans. AGU*, *88*, Fall Meet. Suppl., Abstract T13F-03.

Atwater, B. F. (1987), Evidence for great Holocene earthquakes along the outer coast of Washington state, *Science*, *236*, 942–944, doi:10.1126/science.236.4804.942.

Brodsky, E. E., and J. Mori (2007), Creep events slip less than ordinary earthquakes, *Geophys. Res. Lett.*, *34*, L16309, doi:10.1029/2007GL030917.

Brown, K. M., M. D. Tryon, H. R. DeShon, L. M. Dorman, and S. Y. Schwartz (2005), Correlated transient fluid pulsing and seismic tremor in the Costa Rica subduction zone, *Earth Planet. Sci. Lett.*, *238*, 189–203, doi:10.1016/j.epsl.2005.06.055.

Brudzinski, M., E. Cabral-Cano, F. Correa-Mora, C. DeMets, and B. M. Marquez-Azua (2007), Slow slip transients along the Oaxaca subduction segment from 1993 to 2007, *Geophys. J. Int.*, *171*, 523–538.

DeMets, C. (1995), A reappraisal of seafloor spreading lineations in the Gulf of California: Implications for the transfer of Baja California to the Pacific Plate and estimates of Pacific-North America motion, *Geophys. Res. Lett.*, *22*, 3545–3548, doi:10.1029/95GL03323.

Douglas, A., J. Beavan, L. Wallace, and J. Townend (2005), Slow slip on the northern Hikurangi subduction interface, New Zealand, *Geophys. Res. Lett.*, *32*, L16305, doi:10.1029/2005GL023607.

Dragert, H., R. D. Hyndman, G. C. Rogers, and K. Wang (1994), Current deformation and the width of the seismogenic zone of the northern Cascadia subduction thrust, *J. Geophys. Res.*, *99*, 653–668, doi:10.1029/93JB02516.

Dragert, H., K. Wang, and T. S. James (2001), A silent slip event on the deeper Cascadia subduction interface, *Science*, *292*, 1525–1528, doi:10.1126/science.1060152.

Dragert, H., K. Wang, and G. Rogers (2004), Geodetic and seismic signatures of episodic tremor and slip in the northern Cascadia subduction zone, *Earth Planets Space*, *56*, 1143–1150.

Dragert, H., K. Wang, and H. Kao (2007), Observing episodic slow slip with PBO borehole strainmeters along the northern Cascadia margin, *Eos Trans. AGU*, *88*, Fall Meet. Suppl., Abstract T11F-05.

Efron, B., and R. Tibshirani (1994), *An Introduction to the Bootstrap*, Chapman and Hall, New York.

Flück, P., R. Hyndman, and K. Wang (1997), Three-dimensional dislocation model for great earthquakes of the Cascadia subduction zone, *J. Geophys. Res.*, *102*, 20,539–20,550, doi:10.1029/97JB01642.

Gomberg, J., J. L. Rubinstein, Z. G. Peng, K. C. Creager, J. E. Vidale, and P. Bodin (2008), Widespread triggering of nonvolcanic tremor in California, *Science*, *319*, 173, doi:10.1126/science.1149164.

Heaton, T. H, and H. Kanamori (1984), Seismic potential associated with subduction in the northwestern United States, *Bull. Seismol. Soc. Am.*, *74*, 933–941.

Houston, H. (2007), Scaling of the tremor source, *Eos Trans. AGU*, *88*, Fall Meet. Suppl., Abstract T13F-04.

Ide, S., G. C. Beroza, D. R. Shelly, and T. Uchide (2007a), A scaling law for slow earthquakes, *Nature*, *447*, 76–79, doi:10.1038/nature05780.

Ide, S., D. R. Shelly, and G. C. Beroza (2007b), Mechanism of deep low frequency earthquakes: Further evidence that deep non-volcanic tremor is generated by shear slip on the plate interface, *Geophys. Res. Lett.*, *34*, L03308, doi:10.1029/2006GL028890.

Ide, S., K. Imanishi, Y. Yoshida, G. C. Beroza, and D. R. Shelly (2008), Bridging the gap between seismically and geodetically detected slow earthquakes, *Geophys. Res. Lett.*, *35*, L10305, doi:10.1029/2008GL034014.

Ito, Y., and K. Obara (2006a), Dynamic deformation of the accretionary prism excites very low frequency earthquakes, *Geophys. Res. Lett.*, *33*, L02311, doi:10.1029/2005GL025270.

Ito, Y., and K. Obara (2006b), Very low frequency earthquakes within accretionary prisms are very low stress-drop earthquakes, *Geophys. Res. Lett.*, *33*, L09302, doi:10.1029/2006GL025883.

Ito, Y., K. Obara, K. Shiomi, S. Sekine, and H. Hirose (2006), Slow earthquakes coincident with episodic tremors and slow slip events, *Sci. Express*, *10*(1126), 1–4.

Kao, H., S. J. Shan, H. Dragert, G. Rogers, J. F. Cassidy, and K. Ramachandran (2005), A wide depth distribution of seismic tremors along the northern Cascadia margin, *Nature*, *436*, 841–844, doi:10.1038/nature03903.

Kao, H., P. J. Thompson, G. Rogers, H. Dragert, and G. Spence (2006), An automatic Tremor Activity Monitoring System (TAMS), *Eos Trans. AGU*, *87*(52), Fall Meet. Suppl., Abstract T41A-1544.

Kao, H., P. J. Thompson, G. Rogers, H. Dragert, and G. Spence (2007), Automatic detection and characterization of seismic tremors in northern Cascadia, *Geophys. Res. Lett.*, *34*, L16313, doi:10.1029/2007GL030822.

Kao, H., S. J. Shan, G. Rogers, H. Dragert, K. Wang, and T. Lambert (2008), Spatial-temporal patterns of ETS tremors in northern Cascadia: 10 years of observations from 1997 to 2007, report, Geol. Surv. Can., Ottawa, Ont.

LaRocca, M., K. C. Creager, D. Galluzzo, S. Malone, J. Vidale, J. R. Sweet, and A. G. Wech (2009), Cascadia tremor located near plate interface constrained by S minus P wave times, *Science*, *323*, 620–623, doi:10.1126/science.1167112.

Lawson, C. L., and R. Hanson (1995), *Solving Least Squares Problems*, *Classics Appl. Math. Ser.*, vol. 15, Soc. for Ind. and Appl., Math, Philadelphia, Pa.

McCaffrey, R., A. I. Qamar, R. W. King, R. Wells, G. Khazaradze, C. A. Williams, C. W. Stevens, J. J. Vollick, and P. C. Zwick (2007), Fault locking, block rotation and crustal deformation in the Pacific Northwest, *Geophys. J. Int.*, *169*, 1315–1340, doi:10.1111/j.1365-246X.2007.03371.x.

McCausland, W., S. Malone, and D. Johnson (2005), Temporal and spatial occurrence of deep non-volcanic tremor: From Washington to northern California, *Geophys. Res. Lett.*, *32*, L24311, doi:10.1029/2005GL024349.

Miller, M. M., et al. (1998), Precise measurements help gauge Pacific Northwest's earthquake potential, *Eos Trans. AGU*, *79*(23), 269–275, doi:10.1029/98EO00202.

Miller, M. M., D. J. Johnson, C. M. Rubin, H. Dragert, K. Wang, A. Qamar, and C. Goldfinger (2001), GPS-determination of along-strike variation in Cascadia margin kinematics: Implications for relative plate motion, subduction zone coupling, and permanent deformation, *Tectonics*, *20*(2), 161–176, doi:10.1029/2000TC001224.

Miller, M. M., T. I. Melbourne, D. J. Johnson, and W. Q. Sumner (2002), Periodic slow earthquakes from the Cascadia subduction zone, *Science*, *295*, 2423, doi:10.1126/science.1071193.

Mitchell, C. E, P. Vincent, R. J. I. Weldon, and M. A. Richards (1994), Present-day vertical deformation of the Cascadia margin, Pacific Northwest, United States, *J. Geophys. Res.*, *99*, 12,257–12,277, doi:10.1029/94JB00279.

Nadeau, R. M., and D. Dolenc (2005), Nonvolcanic tremors deep beneath the San Andreas Fault, *Science*, *307*, 389, doi:10.1126/science.1107142.

Obara, K (2002), Nonvolcanic deep tremor associated with subduction in southwest Japan, *Science*, *296*, 1679–1681, doi:10.1126/science.1070378.

Peterson, C., D. Christensen, and S. McNutt (2007), Nonvolcanic tremor in south-central Alaska and its relation to the 1998–2000 slow slip event, *Eos Trans. AGU*, *88*, Fall Meet. Suppl., Abstract T11F-08.

Rogers, G., and H. Dragert (2003), Episodic tremor and slip on the Cascadia subduction zone: The chatter of slow earthquakes, *Science*, *300*, 1942–1943.

Rubinstein, J. L., J. E. Vidale, J. Gomberg, P. Bodin, K. C. Creager, and S. D. Malone (2007), Non-volcanic tremor driven by large transient shear stresses, *Nature*, *448*, 579–582, doi:10.1038/nature06017.

Satake, K., K. Shimazaki, Y. Tsuji, and K. Ueda (1996), Time and size of a giant earthquake in Cascadia inferred from Japanese tsunami records of January 1700, *Nature*, *379*, 246–249, doi:10.1038/379246a0.

Savage, J. C., M. Lisowski, and W. H. Prescott (1991), Strain accumulation in western Washington, *J. Geophys. Res.*, *96*, 14,493–14,507, doi:10.1029/91JB01274.

Shelly, D. R., G. C. Beroza, S. Ide, and S. Nakamula (2006), Low-frequency earthquakes in Shikoku, Japan, and their relationship to episodic tremor and slip, *Nature*, *442*, 188–191, doi:10.1038/nature04931.

Shelly, D. R., G. C. Beroza, and S. Ide (2007), Non-volcanic tremor and low-frequency earthquake swarms, *Nature*, *446*, 305–307, doi:10.1038/nature05666.

Sweet, J. R., K. C. Creager, J. E. Vidale, A. Ghosh, M. L. Nichols, and T. L. Pratt (2008), Low-frequency earthquakes in Cascadia using Texan array, *Eos Trans. AGU*, Fall Meet. Suppl., Abstract U33A-0024, in press.

Szeliga, W., T. Melbourne, M. M. Miller, and V. M. Santillan (2004), Southern Cascadia episodic slow earthquakes, *Geophys. Res. Lett.*, *31*, L16602, doi:10.1029/2004GL020824.

Szeliga, W., T. Melbourne, V. M. Santillan, and M. M. Miller (2008), GPS constraints on 34 slow slip events in the Cascadia subduction zone, 1997–2005, *J. Geophys. Res.*, *113*, B04404, doi:10.1029/2007JB004948.

Wang, K., R. Wells, S. Mazzoti, R. D. Hyndman, and T. Sagiya (2003), A revised dislocation model of interseismic deformation of the Cascadia subduction zone, *J. Geophys. Res.*, *108*(B1), 2026, doi:10.1029/2001JB001227.

Wang, K., H. Dragert, H. Kao, and E. Roeloffs (2008), Characterizing an "uncharacteristic" ETS event in northern Cascadia, *Geophys. Res. Lett.*, *35*, L15303, doi:10.1029/2008GL034415.

Wech, A. G., and K. C. Creager (2007), Cascadia tremor polarization evidence for plate interface slip, *Geophys. Res. Lett.*, *34*, L22306, doi:10.1029/2007GL031167.

Wech, A. G., and K. C. Creager (2008), Automated detection and location of Cascadia tremor, *Geophys. Res. Lett.*, *35*, L20302, doi:10.1029/2008GL035458.

————————————

A. C. Aguiar, T. I. Melbourne, and C. W. Scrivner, Department of Geological Sciences, Central Washington University, Ellensburg, WA 98926, USA. (aguiara@geology.cwu.edu)